IIETA International Information and Engineering Technology Association
Advancing the World of Information and Engineering

Mathematical Modelling of Engineering Problems
Vol. 12, No. 8, August, 2025, pp. 2908-2916
Journal homepage: http://iieta.org/journals/mmep

AC Dielectric Strength of Polyethylene Terephthalate Under Thermal Aging

Mohammed Nedjar*, Zohra Ait-Saadi

Laboratoire de Génie Electrique, Université Mouloud Mammeri, Tizi-Ouzou 15000, Algeria

Corresponding Author Email: mohammed.nedjar@ummto.dz

https://doi.org/10.18280/mmep.120832

Received: 6 April 2025
Revised: 18 July 2025
Accepted: 25 July 2025
Available online: 31 August 2025

Keywords:
polyethylene terephthalate, thermal aging, breakdown, dielectric strength, Fournier Transform Infrared (FTIR), Thermogravimetric Analysis (TGA)

ABSTRACT

This paper reports the AC dielectric strength of polyethylene terephthalate subjected to thermal aging. The aging was conducted for 8500, 6000, 4000 and 3000 hours at 130, 140, 150 and 160°C, respectively. The insulation, of 200 µm thickness, was shaped by a film sandwiched between two sheets. Square specimens, with a side length of 7.5 cm, were prepared. Virgin and aged specimens were subjected to AC dielectric breakdown. The material was analyzed using Fourier Transform Infrared (FTIR) and Thermogravimetric Analysis (TGA). The investigation reveals changes of dielectric strength versus aging time. The lessening is attributed to the increase in mean free path, which leads to the increase of charge carrier mobility. While, its increase is attributed to the reduction of charge carrier mobility. The dielectric strength is linked to the presence of defects. FTIR analysis indicates a decrease in the peak intensities of the infrared absorbance bands after aging. Furthermore, some absorbance bands disappeared after aging. The TGA thermograms exhibit an alteration of onset temperature and residues. A colour change and increased brittleness were noticed. The thermal degradation is accompanied by the formation of non-volatile residue consisting of interconnected aromatic rings. To determine the thermal lifetime of the dielectric material, additional tests over longer durations must be conducted.

1. INTRODUCTION

Polyethylene terephtalate (PET) is widely employed in industry [1] because of its good mechanical properties, low water absorption and resistance to inorganic chemicals [2]. Yang et al. [3] presented the properties of PET: glass transition temperature T_g=80°C, melting point T_m=258°C, density ρ=1.40 g/cm^3, relative permittivity at 50 Hz ε_r=3.1 and hygroscopicity h=0.4% Despite of its advantages, PET degrades under thermal aging.

Panowicz et al. [2] examined the properties of PET after thermo-oxidative aging. Sheets of the material were aged in oven heated at 140°C in such a way that air could freely flow around the samples. Specimens were withdrawn from the oven after 21, 35 and 56 days. The study shows that the quantity of the crystalline phase raises by about 8%. The glass transition and melt temperatures heighten with aging time. The tests point a raise of Young's modulus and a shortening of elongation at rupture for the temperature range between 25 and 75°C. A change in fracture character of the insulation from ductile to brittle was noticed.

Samperi et al. [4] considered thermal aging of PET at the temperature between 270 and 370°C. The authors reported that cyclic oligomers are formed but decompose at higher temperature. Whereas the formation of anhydride containing-oligomers is well apparent. Acetaldehyde was detected in aged specimens.

McNeill and Bounekhel [5] conducted thermal stabilities of PET by thermogravimetry and thermal volatilisation analysis. The authors exhibited that the initial scission happens at the ester linkage to give terminal carboxyl and vinyl structures in the chains. For all the temperatures at which volatile products are released, carbone monoxide and carbone dioxide are formed.

Bárány et al. [6] viewed the influence of thermal aging on sheets of PET with about 0.3 mm thickness. The aging was realized, at just above the glass transition temperature, until 264 h. The researchers displayed that the aging causes an increase of Yield stress and an embrittlement of the samples.

Chipara et al. [7] reported the thermooxidative degradation of PET at 125 and 150°C. The authors pointed a decrease of elongation at break and tensile strength versus aging time. At 150°C, a transition from crosslinking to chain scissions was noted after 500 h. It was noticed that the glass transition temperature varies in function of aging time at 125°C. The researchers closed that the thermooxidative decomposition is governed by a first - order process.

For the use of an insulating material in a device, it is necessary to study the effect of thermal aging on its properties. It is useful to determine the temperature index which is the temperature corresponding to a lifetime of 20000 h. The goal of the present work is to investigate the evolution of dielectric strength of PET under thermal aging. The PET was characterised by Fourier Transform Infrared (FTIR) and Thermogravimetric Analysis (TGA).

2. EXPERIMENTAL TECHNIQUES

2.1 Sample preparation

PET was supplied in the form of rollers with 200 µm thickness. The insulation is extensively used in electrical machines. The material is shaped by a film stuck between two sheets. The last protect the film inside the machine slots. For the experiments, square samples, of 7.5 cm in side, were carried out. To avert the presence of defects, the specimens were verified with a microscope. The presence of defects can generate partial discharges when the dielectric is subjected to electric stress.

2.2 Thermal aging

The prepared samples were placed in ventilated ovens regulated at 130, 140, 150 and 160°C up to 8500, 6000, 4000 and 3000 h, respectively. After each interval of 500 h, 3 samples were deducted from the ovens.

2.3 Dielectric testing

Before dielectric testing, the samples were put in desiccators, during at least 24 h. This step allows eliminating the presence of moisture (drying).

For the breakdown tests, we employed a cell containing two circular plane electrodes made by stainless steel. One electrode has (25 ± 1) mm diameter and approximately 15 mm high. The other electrode has (75 ± 1) mm diameter and approximately 15 mm high [8].

To avoid bypasses, the tank was filled by a mineral oil: "BORAK 22". Firstly, the tested specimen was sandwiched between the electrodes. Then, AC voltage ramp of 0.5 kV/s, provided by high voltage transformer, was applied to the sample until the failure happened. The experiments were achieved at ambient temperature. After rupture, the breakdown voltage was registered and the thickness of the insulation, at the failure point, was measured. The dielectric strength was calculated as the ratio of the breakdown voltage to the thickness. When black particles due to the electrical breakdown were observed, the oil was filtered.

2.4 Fournier transform infrared (FTIR)

For the achievement of the infrared spectra, a dust of the insulating material was blended with a potassium bromide quantity (KBr). The mixture was pressed, and then the pellets were elaborated. The measurements of the spectra were archieved with JASCO FT/IR equipment in wavenumber range 4000 - 400 cm^{-1}. The device was linked to a computer.

2.5 Thermogravimetric analysis

TGA was accomplished with NETZSCH STA 409 PC/PG at temperatures varying between 25 and 800°C under nitrogen atmosphere. A small amount of the polymer was withdrawn and put in the crucible of the apparatus micro-balance. The warming rate is 10°C/min and programmed with a computer. The mean mass of the taken amount is about 5 mg. The equipment was connected to a computer.

3. RESULTS AND DISCUSSION

3.1 Change of dielectric strength against aging time

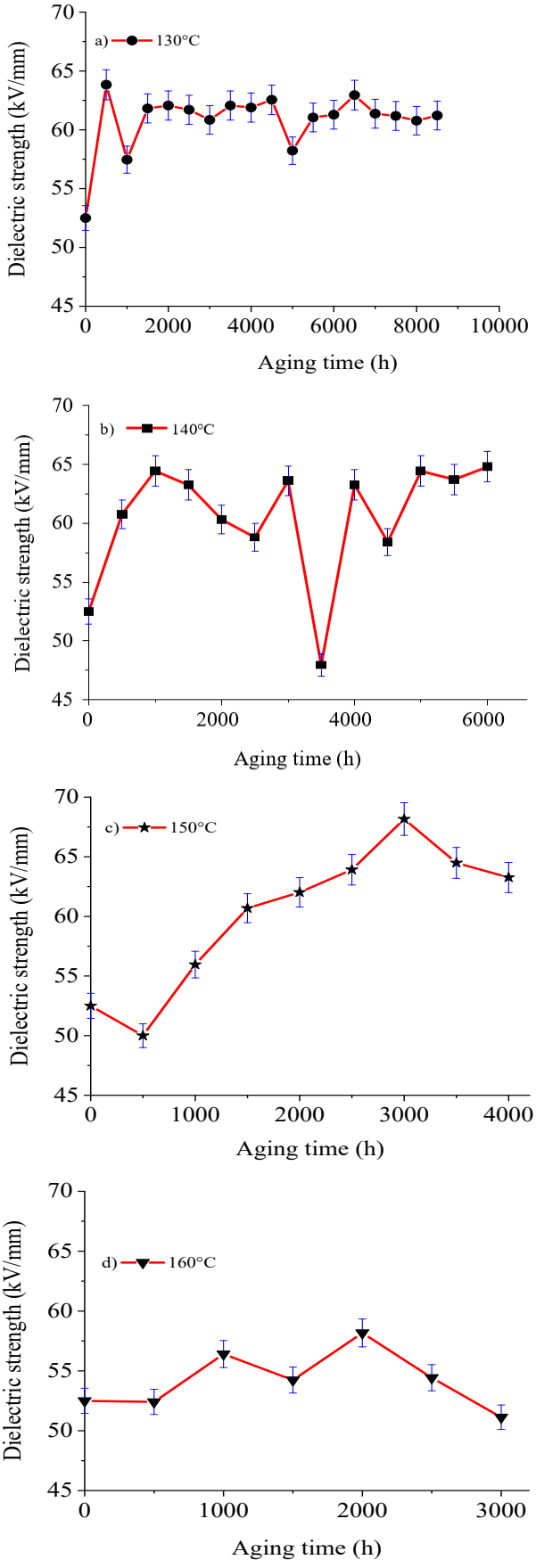

Figure 1. Dielectric strength versus aging time a) at 130°C; b) at 140°C; c) at 150°C; d) at 160°C

Figure 1 illustrates the change of dielectric strength (E_b) with respect to aging time at different temperatures. The change can be depicted as below:

- At 130℃, E_b increases rapidly from 52.50 kV/mm to 63.83 kV/mm, lowers to 57.46 kV/mm and rises until 61.82 kV/mm after 1500 h. Next E_b lessens slowly to 60.84 kV/mm for 3000 h. Then E_b increases a little to 62.06 kV/mm, diminishes slightly until 61.89 kV/mm and grows to 62.55 kV/mm for 4500 h. Later E_b reduces to 58.23 kV/mm, raises to 62.95 kV/mm and decays to 60.77 kV/mm then enlarges somewhat to 61.21 kV/mm after 8500 h. The maximum modification is 21.58%.
- At 140℃, E_b grows quickly from 52.50 kV/mm to 64.44 kV/mm and decays until 58.79 kV/mm for 2500 h. After E_b heightens to 63.60 kV/mm, falls to 47.97 kV/mm and raises quickly until 63.26 kV/mm after 4000 h. After E_b lowers to 58.41 kV/mm, enhances to 64.42 kV/mm and weakens to 63.71 kV/mm then it rises a rather to 64.78 kV/mm for 6000 h. The maximum changing is 23.39%.
- At 150℃, E_b lowers slowly from 52.50 kV/mm to 50.00 kV/mm, raises quickly until 68.16 kV/mm and shortens again to 63.26 kV/mm after 4000 h. The maximum change is 29.83%.
- At 160℃, at first E_b is practically constant; its value is about 52.50 kV/mm. Then it increases to 56.41 kV/mm and lowers until 54.23 kV/mm for 1500 h. Beyond this time, E_b raises to 58.17 kV/mm and drops to 51.13 kV/mm after 3000 h. The maximum variation is 10.82%.

Table 1(a). Mean and error bars of E_b before and after aging at 130℃

Aging Time (h)	Mean (kV/mm)	Error Bars (kV/mm)
0	52.500	1.050
500	63.830	1.276
1000	57.460	1.149
1500	61.818	1.236
2000	62.063	1.241
2500	61.702	1.234
3000	60.842	1.216
3500	62.063	1.241
4000	61.895	1.237
4500	62.553	1.251
5000	58.228	1.164
5500	61.047	1.220
6000	61.283	1.225
6500	62.947	1.258
7000	62.368	1.227
7500	61.179	1.223
8000	60.773	1.215
8500	61.211	1.224

Table 1(b). Mean and error bars of E_b after aging at 140℃

Aging Time (h)	Mean (kV/mm)	Error Bars (kV/mm)
500	60.749	1.214
1000	64.444	1.288
1500	63.243	1.264
2000	60.317	1.206
2500	58.794	1.175
3000	63.602	1.272
3500	47.967	0.959
4000	63.262	1.265
4500	58.407	1.168
5000	64.420	1.288
5500	63.710	1.274
6000	64.778	1.295

Table 1(c). Mean and error bars of E_b after aging at 150℃

Aging Time (h)	Mean (kV/mm)	Error Bars (kV/mm)
500	50.000	1.000
1000	55.959	1.119
1500	60.684	1.213
2000	62.021	1.240
2500	63.913	1.278
3000	68.161	1.363
3500	64.486	1.289
4000	63.262	1.265

Table 1(d). Mean and error bars of E_b after aging at 160℃

Aging Time (h)	Mean (kV/mm)	Error Bars (kV/mm)
500	52.410	1.048
1000	56.410	1.128
1500	54.233	1.084
2000	58.173	1.163
2500	54.430	1.088
3000	51.126	1.022

Table 2(a). Standard deviation of E_b before and after aging at 130℃

Aging Time (h)	Standard Deviation (kV/mm)
0	3.88
500	4.94
1000	5.41
1500	2.65
2000	1.46
2500	2.84
3000	3.00
3500	2.19
4000	4.03
4500	2.91
5000	4.49
5500	3.29
6000	7.23
6500	1.26
7000	6.49
7500	4.74
8000	4.21
8500	1.22

Table 2(b). Standard deviation of E_b after aging at 140℃

Aging Time (h)	Standard Deviation (kV/mm)
500	4.61
1000	2.63
1500	7.44
2000	3.33
2500	2.01
3000	2.62
3500	2.01
4000	8.22
4500	4.95
5000	1.79
5500	1.81
6000	4.51

Table 2(c). Standard deviation of E_b after aging at 150℃

Aging Time (h)	Standard Deviation (kV/mm)
500	2.20
1000	3.22
1500	4.76
2000	3.84
2500	6.22
3000	1.25
3500	4.23
4000	3.13

Table 2(d). Standard deviation of E_b after aging at 160°C

Aging Time (h)	Standard Deviation (kV/mm)
500	3.52
1000	3.05
1500	6.66
2000	4.77
2500	3.48
3000	4.41

- The mean, standard deviation and error bars of E_b were calculated. The results are presented in the Tables 1-2.

3.2 Modification in sample colour

Figure 2 shows the insulation before and after aging. As it can be seen, the PET color changed after aging.

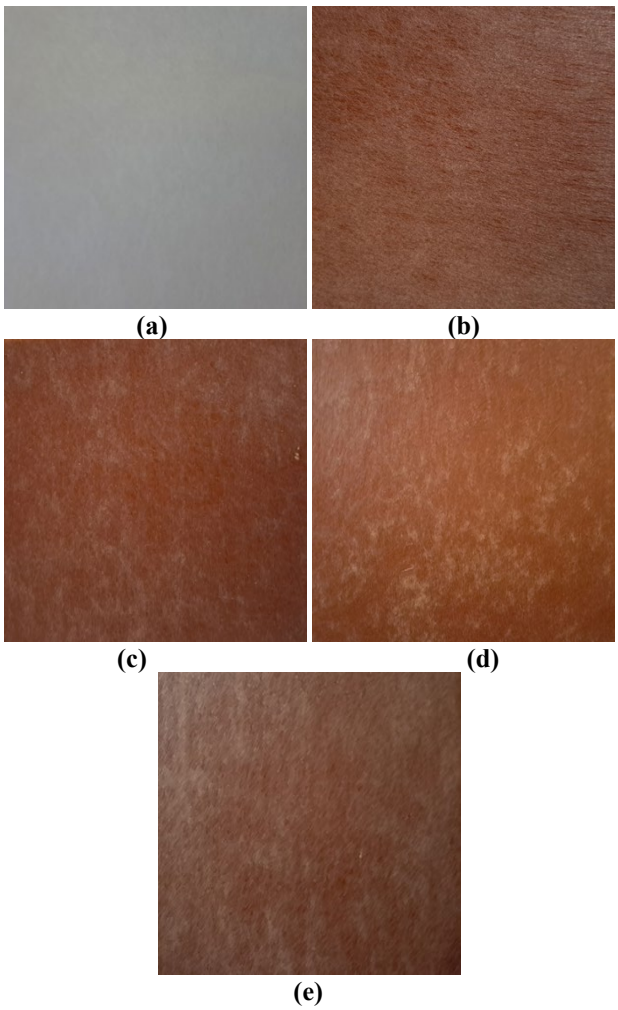

Figure 2. Photographs of the polymer: a) Before aging; b) After 8500 h at 130°C; c) After 6000 h at 140°C; d) After 4000 h at 150°C; e) After 3000 h at 160°C

3.3 FTIR analysis

3.3.1 Before aging

Table 3 presents the significant infrared (IR) absorbance bands of PET ascribed to the vibrations as yielded by Chércoles Asensio et al. [9].

Figure 3(a) shows the IR spectrum before aging. This spectrum can be summarized as follows:

- It was detected an absorbance band at 1710 cm^{-1} ascribed to stretching vibration of C=O, characteristic of ester.
- The absorbance bands, noticed at 1408 and 1344 cm^{-1}, are related to symmetric and asymmetric bending vibration in-plane C−H and rocking bending of C – H − CH_2−.
- The absorbance band, shown at 1238 cm^{-1}, is allocated to the stretching vibration of C− C (O) − O.
- The absorbance band, arising at 1097 cm^{-1}, is due to the stretching vibration of – O – C –.
- Two absorbance bands are identified at 1017 and 962 cm^{-1} corresponding to the bending vibration in-plane of =C − H.
- The bending vibration out-of-plane of =C − H occurs at 872 cm^{-1}.
- The absorbance band, emerging at 717 cm^{-1}, matches to the wagging bending vibration of =C − H.

Table 3. Infrared absorbance bands

Absorbance Band Number	Wavenumber (cm^{-1})
1	1710
2	1408
3	1344
4	1238
5	1097
6	1017
7	962
8	872
9	717

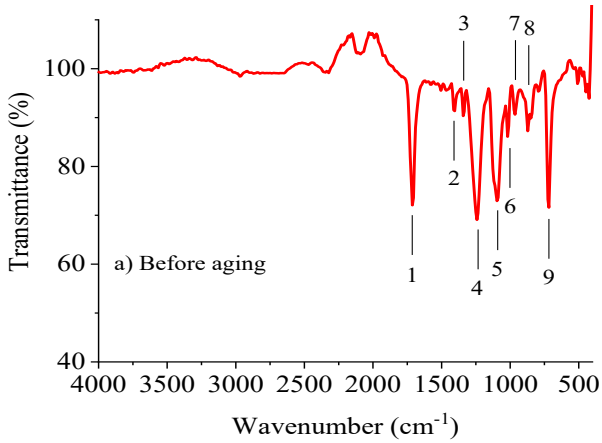

Figure 3(a). IR spectrum before aging

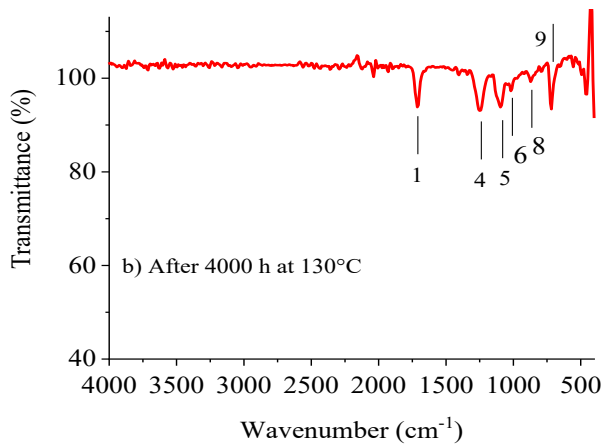

Figure 3(b). IR spectrum after 4000 h at 130°C

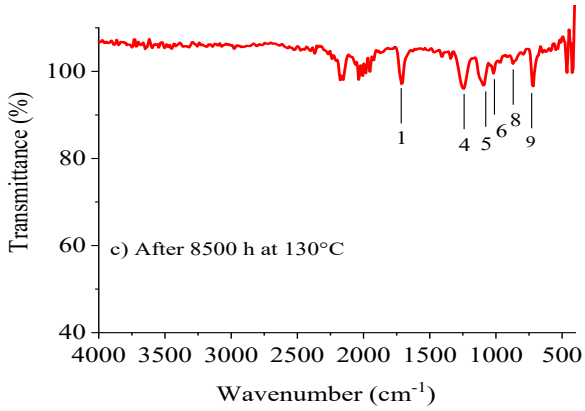

Figure 3(c). IR spectrum after 8500 h at 130°C

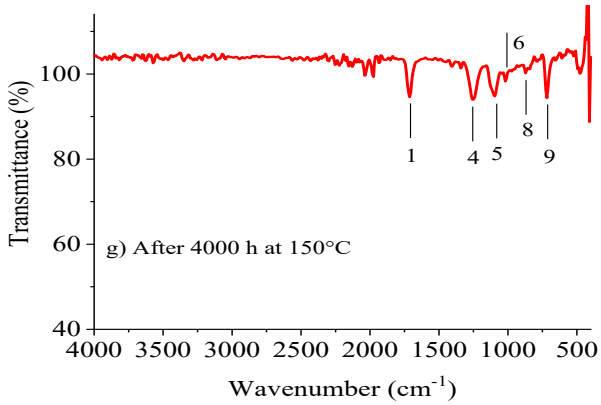

Figure 3(g). IR spectrum after 4000 h at 150°C

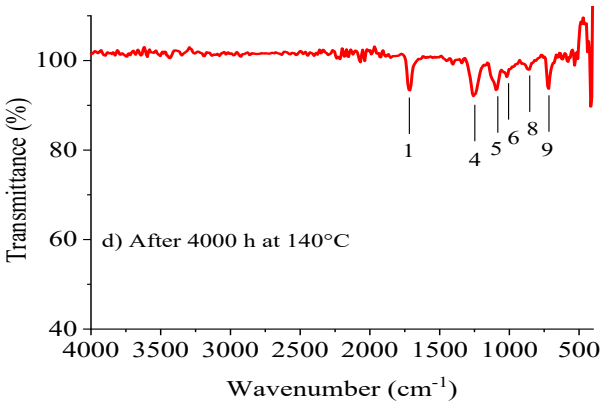

Figure 3(d). IR spectrum after 4000 h at 140°C

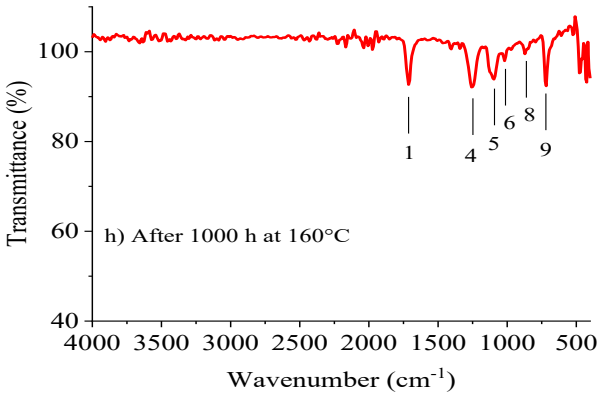

Figure 3(h). IR spectrum after 1000 h at 160°C

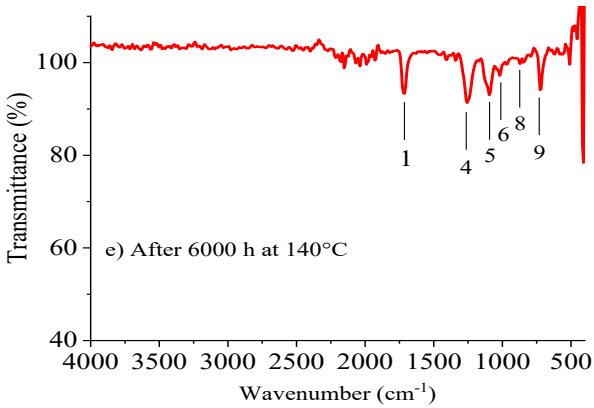

Figure 3(e). IR spectrum after 6000 h at 140°C

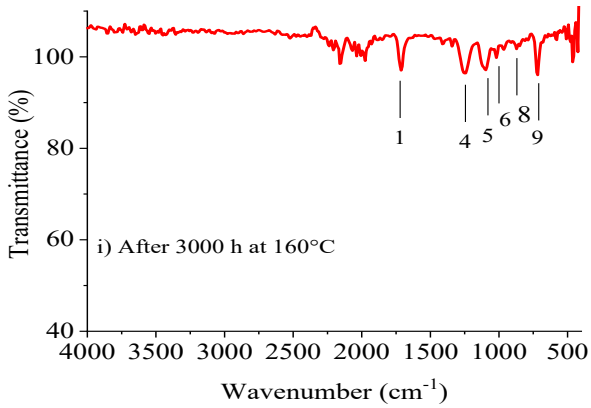

Figure 3(i). IR spectrum after 3000 h at 160°C

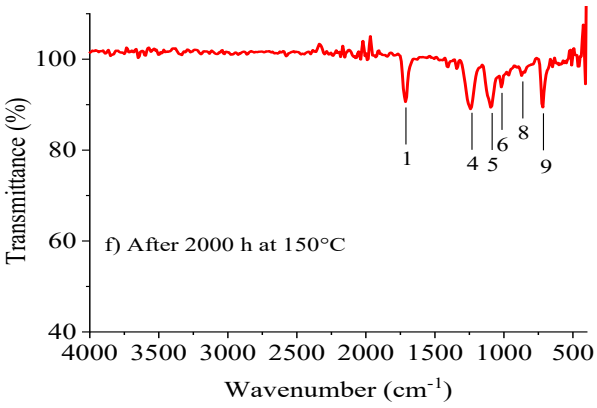

Figure 3(f). IR spectrum after 2000 h at 150°C

3.3.2 After aging

Figures 3(b)-(i) represent the IR spectra after aging. As one can notice, the peak intensities of absorbance bands at 1710, 1238, 1097, 1017, 872 and 717 cm^{-1}, decreased. Furthermore, we remark that the absorbance bands at 1408, 1344 and 962 cm^{-1} vanished.

3.4 TGA thermograms

As one can observe, the TGA thermograms have the same form. Between 25°C and 300°C, a mass loss of about 1% was remarked before and after aging. This mass loss is assigned to the evaporation of water and volatile solvents.

3.4.1 Before aging

Figure 4(a) shows the thermogravimetric curve before

aging. At the beginning, the mass loss begins at around 402°C, expedites and reaches 94% at 457°C. Next, the mass slackens and it remains a residue of 5.3% at 797°C. The temperature matching to 50% mass loss is 432°C.

3.4.2 After aging

Figures 4(b)-(i) give the TGA thermograms after aging.

a) Aging at 130°C

- After 4000 h at 130°C, the mass loss starts at around 394°C, accelerates and attains 86.45% at 453°C. After the mass loss slackens and it stays a remainder of 12.93% at 796°C. The temperature corresponding to 50% mass loss is 430°C.
- After 8500 h at 130°C, the mass loss begins at around 395°C. Beyond the onset temperature, it hastens and reaches 80.74% at 455°C. After, the mass loss slows down and it remains a residual of 17.83% at 796°C. The 50% mass loss is attained at 432°C.

b) Aging at 140°C

- After 4000 h at 140°C, the mass loss initiates at around 396°C and hastens to 81.30% at 454°C. After the mass loss slackens and it keeps a residuum of 15.90% at 793°C. The 50% mass loss is attained at 431°C.
- After 6000 h at 140°C, the mass loss starts at around 404°C, expedites and achieves 86.45% at 455°C. Latter the mass loss goes down and it remains a remainder of 14.06% at 796°C. The temperature matching to 50% mass loss is 430°C.

c) Aging at 150°C

- After 2000 h at 150°C, the mass loss begins at around 399°C and accelerates up to 81.00% at 454°C. After, the mass loss decelerates and it remains a residue of 17.52% at 794 °C. The 50% mass loss is attained at 434°C.
- After 4000 h at 150°C, the mass loss starts at around 398°C and hastens to 83.84% at 453°C. Latter the mass loss decelerates and it keeps a residue of 14.35% at 793°C. The temperature corresponding to 50% mass loss is 432°C.
- After 1000 h at 160°C, the mass loss begins at around 403°C and speeds up to 87.23% at 452°C. After, the mass loss slackens and it stays a residual of 11.40% at 792°C. The 50% mass loss is reached at 431°C.

d) Aging at 160°C

- After 3000 h at 160°C, the mass loss initiates at around 397°C and hastens to 87.44% at 456°C. Latter it slackens and it remains a residuum of 12.22% at 792°C. The temperature matching to 50% mass loss is 429°C.

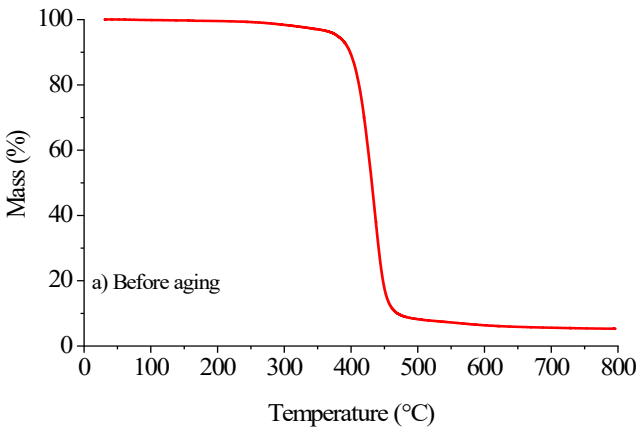

Figure 4(a). TGA thermogram before aging

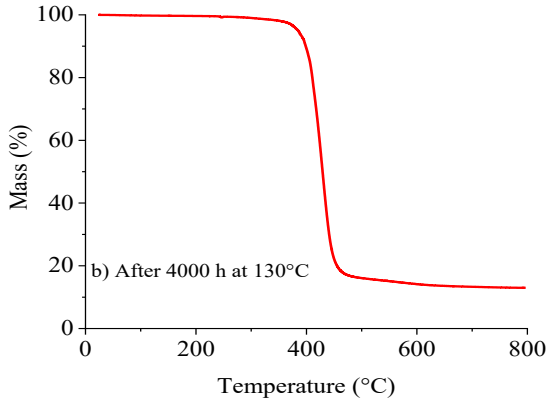

Figure 4(b). TGA thermogram after 4000 h at 130°C

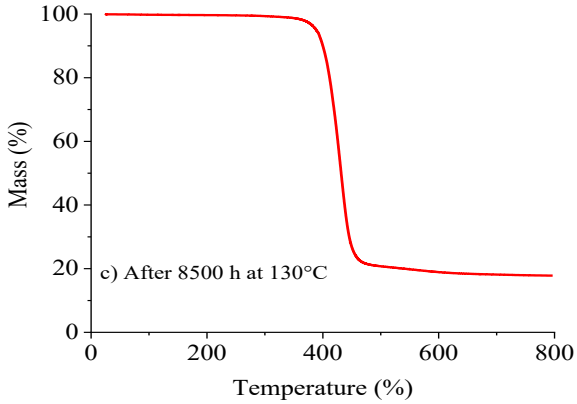

Figure 4(c). TGA thermogram after 8500 h at 130°C

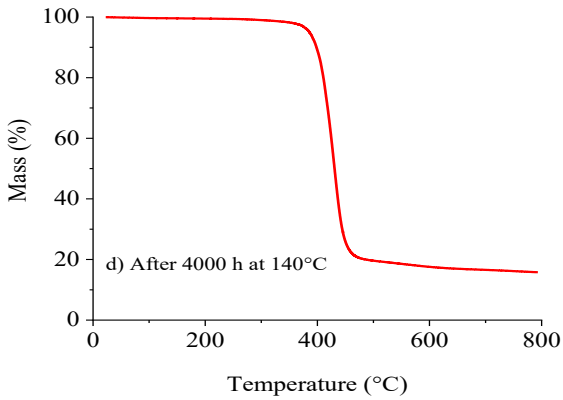

Figure 4(d). TGA thermogram after 4000 h at 140°C

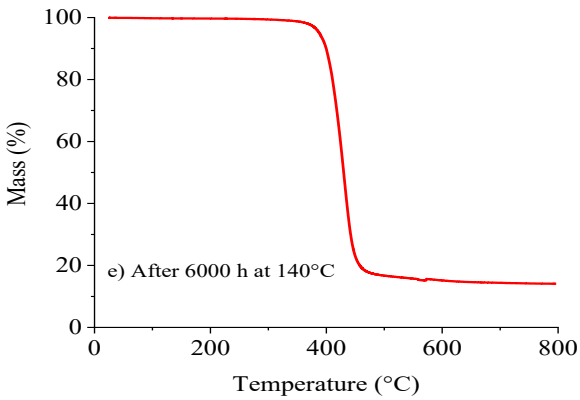

Figure 4(e). TGA thermogram after 6000 h at 140°C

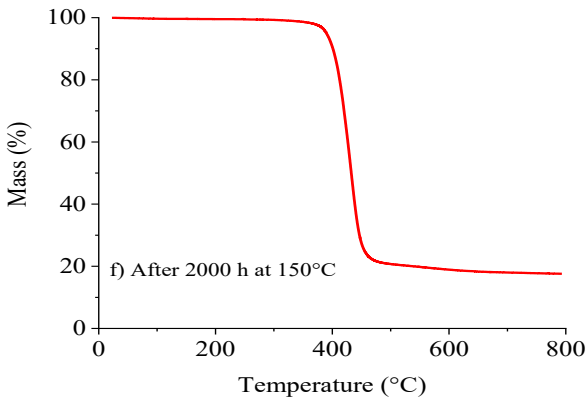

Figure 4(f). TGA thermogram after 2000 h at 150°C

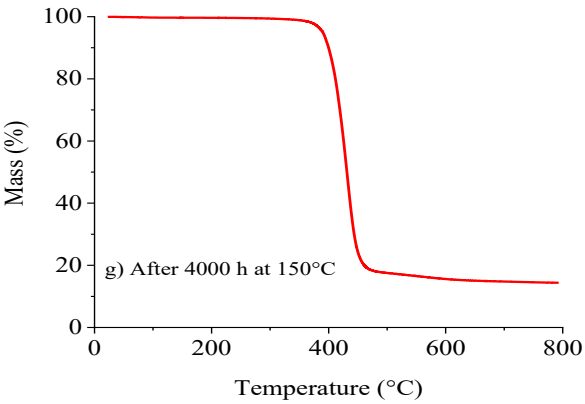

Figure 4(g). TGA thermogram after 4000 h at 150°C

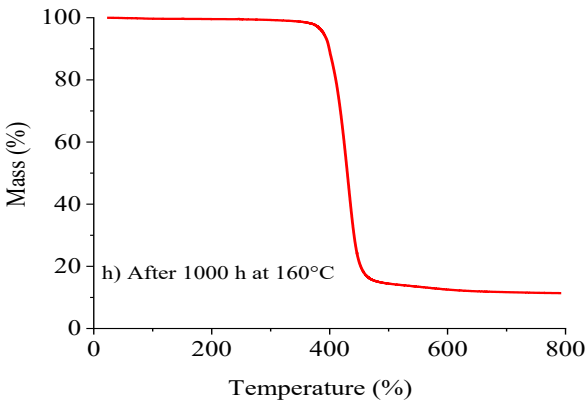

Figure 4(h). TGA thermogram after 1000 h at 160°C

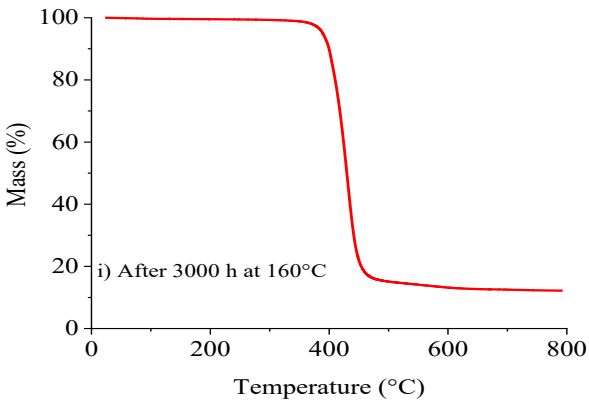

Figure 4(i). TGA thermogram after 3000 h at 160°C

3.5 Discussion

(a) The aging heightens the thermal agitation producing a progressive lowering in the viscosity. Thereby the molecular bonds decay and the free volume grows. Consequently, the mean free path of charge carriers increases causing the raise of their mobility. This phenomenon explains the shortening of E_b. In the contrary, the enlargement of dielectric strength is ascribed to the rearrangement in the molecular chains inducing a shortening in the mean free path and the mobility of charge carriers. This phenomenon was reported elsewhere [10]. Xing et al. [11] pointed out the growth of the free volume in polypropylene with respect to temperature. The free volume increases from 1.23 $\times 10^{-9} m^3$ at 25°C to 1.56 $\times 10^{-9}$ m^3 for 90°C.

(b) Statistical study indicates that the mean of E_b is ranged from 47.97 to 68.16 kV/mm. The error bars are situated between 0.959 and 1.363 kV/mm. The standard deviation varies between 1.22 and 8.22 kV/mm.

(c) Figure 1(b) presents a maximum of 64.44 kV/mm, after 1000 h, which may be due to the crystallization. The curve shows also a minimum of 47.97 kV/mm, after 4500 h, which may be assigned to the chain scission.

(d) For all temperatures, the sample colour changed after aging. Moreover, the dielectric material became brittle after aging. During the heating, we remarked a decrease in the adhesion of the film to the sheets.

(e) Dielectric strength is affected by the presence of defects which can exist within the polymer during the making or created by the aging. Katsuta et al. [12] indicated that breakdown strength of XLPE cables decreases versus void size. Hagen and Ildstad [13] established that the addition of conducting iron and copper particles to XLPE insulation shortens AC dielectric strength from 107 kV/mm to 70 kV/mm and 35 kV/mm, for spherically and irregularly shaped particles respectively. For the samples holding glass particles, the dielectric strength diminishes to 55 kV/mm independently to the form of particles. Chen and Davies [14] examined the behaviour of low-density polyethylene under DC electric stress. The authors reported that, after aging, the samples pointed out oxidation degradation around the defects due to the enhancement of electric field.

(f) The meaning infrared absorbance bands, listed in Table 3, were reported elsewhere [15-18]. After aging, a diminution in the intensities of absorbance band peaks was noted. In addition, an extinction of some absorbance bands was observed. The FTIR peak loss may be attributed to the chain scission and the decrease of molar mass as reported by Oreski et al. [19] This phenomenon leads to the increase of the dielectric strength. For a fixed temperature, the residue trends to increase versus aging time. Besides, E_b tends to raise against heating time. The rate of reactions can be given by [20]:

$$r = \frac{\partial \propto}{\partial t} = Aexp(-\frac{E}{RT})(1-\alpha)^n \quad (1)$$

$$\propto = \frac{\omega_0 - \omega}{\omega_0 - \omega_f} \quad (2)$$

where, α is a conversion, t is the time, A is the pre-exponential factor, E is the activation energy, R is universal gas constant,

T is temperature, and ω_0, ω, ω_f are the weight of the sample at initial time (t=0), time t and at the end of the TGA experiment, respectively, and n is the reaction order.

The dielectric strength depends on the molar mass and the chain scission. Thence it is linked to the thermal degradation kinetics.

(g) The TGA thermograms exhibit that the decomposition of the polymer takes place depending on one stage: the process is governed by a first-order chemical reaction. This phenomenon was reported elsewhere [15, 21]. The graphs display modifications of onset temperature and residue. The beginning temperature varies between 394°C and 404°C. The residue alters from 5.3% to 17.83%.

(h) PET degradation involves ester hydrolysis and thermo-oxidation. Holland and Hay [22] related thermal degradation of PET. The authors showed that the presence of diethylene glycol and isophthalate units has a significant influence on the process, increasing the chain flexibility and creating more favourable bond angles. The thermal degradation causes the formation of non-volatile residue contained almost exclusively of interconnected aromatic rings.

(i) Complementary tests, at longer times of heating, are useful to determine thermal endurance curve of PET. The lifetime will be established for a 50% decrease of dielectric strength for all the temperatures, which determines the temperature index.

4. CONCLUSIONS

This investigation allows deducing the following points:

1) AC dielectric strength alters versus aging time. The raise is attributed to the lowering of mean free path and the mobility of charge carriers. On the other hand, its weakening is assigned to the growth of the mean free path and the mobility of charge carriers.
2) A changing in the colour and an embrittlement of the polymer were noticed.
3) The FTIR analysis shows a decrease in the peak intensities of absorbance bands after heating. This phenomenon is allocated to the chain scission and the diminution of the molar mass. Furthermore, the absorbance bands at 1408, 1344 and 962 cm^{-1} disappeared.
4) TGA points that all the thermogram curves have the same shape. Thermal aging changes the onset temperature of decomposition and the remainder. The degradation occurs by one stage: the process is governed by a first-order chemical reaction.
5) The degradation of the insulation produces the formation of non-volatile residue included almost exclusively of interconnected aromatic rings.

REFERENCES

[1] Planes, E., Yrieix, B., Bas, C., Flandin, L. (2014). Chemical degradation of the encapsulation system in flexible PV panel as revealed by infrared and Raman microscopies. Solar Energy Materials and Solar Cells, 122: 15-23. https://doi.org/10.1016/j.solmat.2013.10.033

[2] Panowicz, R., Konarzewski, M., Durejko, T., Szala, M., Lazińska, M., Czerwińska, M., Prasula, P. (2021), Properties of polyethylene terephtalate (PET) after thermo-oxidative aging, Materials, 14(14): 3833. https://doi.org/10.3390/ma14143833

[3] Yang, P., Tian, F., Ohki, Y. (2014). Dielectric properties of poly (ethylene terephthalate) and poly (ethylene 2, 6-naphthalate). IEEE Transactions on Dielectrics and Electrical Insulation, 21(5): 2310-2317. https://doi.org/10.1109/TDEI.2014.004416

[4] Samperi, F., Puglisi, C., Alicata, R., Montaudo, G. (2004). Thermal degradation of poly (ethylene terephthalate) at the processing temperature. Polymer Degradation and Stability, 83(1): 3-10. https://doi.org/10.1016/S0141-3910(03)00166-6

[5] McNeill, I.C., Bounekhel, M. (1991). Thermal degradation studies of terephthalate polyesters: 1. Poly (alkylene terephthalates). Polymer Degradation and Stability, 34(1-3): 187-204. https://doi.org/10.1016/0141-3910(91)90119-C

[6] Bárány, T., Földes, E., Czigány, T. (2007). Effect of thermal and hygrothermal aging on the plane stress fracture toughness of poly (ethylene terephthalate) sheets. Express Polymer Letters, 1(3): 180-187. http://doi.org/10.3144/expresspolymlett.2007.28

[7] Chipara, M.D., Notingher, P.V., Reyes, J.R., Chipara, M.I. (1998), On the thermooxidative degradation of polyethylene terephthalate. In Proceedings on the 1998 IEEE 6th International Conference on Conduction and Breakdown in Solid Dielectrics, Vasteras, Sweden, pp. 283-285. https://doi.org/10.1109/ICSD.1998.709280

[8] IEC 60243-1. (2013). International Standard: Electric strength of insulating materials-Tests methods, Part 1: Tests at Power Frequencies. International Electrotechnical Commission. https://cdn.standards.iteh.ai/samples/19861/a06c44e60b0d428a9ba07834bcc92fe5/IEC-60243-1-2013.pdf.

[9] Chércoles Asensio, R., San Andrés Moya, M., De la Roja, J.M., Gómez, M. (2009). Analytical characterization of polymers used in conservation and restoration by ATR-FTIR spectroscopy. Analytical and Bioanalytical Chemistry, 395(7): 2081-2096. https://doi.org/10.1007/s00216-009-3201-2

[10] Mohammed, N. (2022). Breakdown behaviour of polyesterimide enamelled wire subjected to thermal aging. Annales de Chimie - Science des Matériaux, 46(3): 163-168. https://doi.org/10.18280/acsm.460308

[11] Xing, Z., Gu, Z., Zhang, C., Guo, S., Cui, H., Lei, Q., Li, G. (2022). Influence of space charge on dielectric property and breakdown strength of polypropylene dielectrics under strong electric field. Energies, 15(12): 4412. https://doi.org/10.3390/en15124412

[12] Katsuta, G., Toya, A., Katakai, S., Kanaoka, M., Sekii, Y. (1991). Influence of defects on insulating properties of XLPE cable. In Proceedings of the 3rd International Conference on Properties and Applications of Dielectric Materials, Tokyo, Japan, pp. 485-489. https://doi.org/10.1109/ICPADM.1991.172103

[13] Hagen, S.T., Ildstad, E. (1993). Reduction of AC-breakdown strength due to particle inclusions in XLPE cable insulation. In 1993 Third International Conference on Power Cables and Accessories 10kV-500kV, London, UK, pp. 165-168.

[14] Chen, G., Davies, A.E. (2002). The influence of defects on the short-term breakdown characteristics and long-term dc performance of LDPE insulation. IEEE Transactions on Dielectrics and Electrical Insulation,

7(3): 401-407. https://doi.org/10.1109/94.848925
[15] Ait-Saadi, Z., Nedjar, M. (2023). Electrical properties of polyethylene terephthalate under hydrothermal aging. Mathematical Modelling of Engineering Problems, 10(1): 63-70. https://doi.org/10.18280/mmep.100108
[16] Djebara, M., Stoquert, J.P., Abdesselam, M., Muller, D., Chami, A.C. (2012). FTIR analysis of polyethylene terephthalate irradiated by MeV He+. Nuclear Instruments and Methods in Physics Research Section B: Beam Interactions with Materials and Atoms, 274: 70-77. https://doi.org/10.1016/j.nimb.2011.11.022
[17] Aljoumaa, K., Abboudi, M. (2016). Physical ageing of polyethylene terephthalate under natural sunlight: Correlation study between crystallinity and mechanical properties. Applied Physics A, 122(1): 6. https://link.springer.com/article/10.1007/s00339-015-9518-0
[18] Dubelly, F., Planes, E., Bas, C., Pons, E., Yrieix, B, Flandin, L. (2017), The hydrothermal degradation of PET in laminated multilayer, European Polymer Journal, 87: 1-13. http://doi.org/10.1016/j.eurpolymj.2016.12.004
[19] Oreski, G., Ottersboeck, B., Barretta, C., Christoefl, P., Radl, S., Pinter, G. (2023). Degradation of PET–quantitative estimation of changes in molar mass using mechanical and thermal characterization methods. Polymer Testing, 125: 108130. https://doi.org/10.1016/j.polymertesting.2023.108130
[20] Chan, J.H., Balke, S.T. (1997). The thermal degradation kinetics of polypropylene: Part III. Thermogravimetric analyses. Polymer Degradation and Stability, 57(2): 135-149. https://doi.org/10.1016/S0141-3910(96)00160-7
[21] Jenekhe, S.A., Lin, J.W., Sun, B. (1983). Kinetics of the thermal degradation of polyethylene terephthalate. Thermochimica Acta, 61(3): 287-299. https://doi.org/10.1016/0040-6031(83)80283-4
[22] Holland, B.J., Hay, J.N. (2002). The thermal degradation of PET and analogous polyesters measured by thermal analysis–Fourier transform infrared spectroscopy. Polymer, 43(6): 1835-1847. https://doi.org/10.1016/S0032-3861(01)00775-3